


Article

Polycarboxylated Eggshell Membrane Scaffold as Template for Calcium Carbonate Mineralization

José L. Arias ^{*}, Karla Silva, Andrónico Neira-Carrillo , Liliana Ortiz, José Ignacio Arias, Nicole Butto and María Soledad Fernández

Faculty of Veterinary and Animal Sciences, University of Chile, Santiago 8820808, Chile; karla.silva@ug.uchile.cl (K.S.); aneira@uchile.cl (A.N.-C.); lbortizm@ug.uchile.cl (L.O.); iarias@uchile.cl (J.I.A.); nbutto@veterinaria.uchile.cl (N.B.); sofernan@uchile.cl (M.S.F.)

* Correspondence: jarias@uchile.cl

Received: 8 August 2020; Accepted: 5 September 2020; Published: 9 September 2020



Abstract: Biomineralization is a process in which specialized cells secrete and deliver inorganic ions into confined spaces limited by organic matrices or scaffolds. Chicken eggshell is the fastest biomineralization system on earth, and therefore, it is a good experimental model for the study of biomineralization. Eggshell mineralization starts on specialized dispersed sites of the soft fibrillar eggshell membranes referred to as negatively charged keratan sulfate mammillae. However, the rest of the fibrillar eggshell membranes never mineralizes, although 21% of their amino acids are acidic. We hypothesized that, relative to the mammillae, the negatively charged amino acids of the fibrillar eggshell membranes are not competitive enough to promote calcite nucleation and growth. To test this hypothesis, we experimentally increased the number of negatively charged carboxylate groups on the eggshell membrane fibers and compared it with in vitro calcite deposition of isolated intact eggshell membranes. We conclude that the addition of poly-carboxylated groups onto eggshell membranes increases the number of surface nucleation sites but not the crystal size.

Keywords: eggshell mineralization; poly-glutamic acid

1. Introduction

Biomineralization is a widespread phenomenon in nature through which living organisms fabricate a large variety of solid organic-inorganic composite structures, such as intracellular crystals in prokaryotes; exoskeletons in protozoa, algae, and invertebrates; spicules; lenses; bone; teeth; statoliths; otoliths; eggshells; and plant mineral structures, as well as pathological biominerals such as gall stones, kidney stones, and oyster pearls [1–8]. In this process, specialized cells secrete and deliver inorganic ions into confined spaces limited by organic matrices or scaffolds. The resulting biominerals are formed in elaborate shapes and hierarchical structures across several length scales by interaction at the organic-inorganic interface, where the rate of crystal formation is regulated by the control of the microenvironment in which such mineralization events take place [9]. Although there are several types of biominerals, the main mineral resulting from biomineralization is calcium carbonate (CaCO₃), specifically the more stable form, calcite. Considering its size, the chicken eggshell is the fastest biomineralization system on earth, where 5 g of calcite are deposited every day on each egg. Therefore, the avian eggshell is a good experimental model for the study of biomineralization.

Structurally, the eggshell is a multilayered calcitic bioceramic built on different organic scaffolds produced by different cells located along defined regions of the avian oviduct in the form of an assembly line [10,11]. The first and innermost scaffolds are the fibrillar eggshell membranes (ESM), which on one hand surround the egg albumen (colloquial: egg white), and on the other hand support discrete accumulations of a different organic composition referred to as mammillae [12]. It has been well

established that the eggshell membranes and mammillae play a crucial role in regulating mineral nucleation and growth by incorporating inorganic precursors, such as ions, ion clusters, and amorphous phases [13–15]; other organic matrices complete the formation of a calcified layer (i.e., palisade) composed of polycrystalline calcite columns that are normal to the eggshell surface [16–18].

Eggshell membrane fibers are composed of mainly type X collagen and other proteins [19–21], and physiologically, they never mineralize in spite of the fact that 21% of their amino acids are acidic (glutamic and aspartic acids) [22]. A review of biomineralization discusses that in other biomineralized systems, such as bone and sea shells, one of the roles of these acidic amino acids is in structural matching for binding ions in a regular array at the surface of an organic matrix [5]. However, there is no differential explanation for additives incorporated in solution or, forming part of a co-polymer or a hydrogel, adsorbed or chemically coupled to a solid scaffold in an inorganic precipitation solution at equivalent saturation concentrations. In particular, eggshell calcite crystal mineralization starts and grows on negatively charged keratan sulfate-rich structures, referred as to mammillae, but not on the surface of the eggshell membrane fibers [23]. We hypothesized that the negatively charged amino acids of the eggshell membrane fibers are not competitive enough to promote calcite nucleation and growth relative to the mammillary sites. To test this hypothesis, we experimentally increased the number of negatively charged carboxylate groups on the eggshell membrane fibers and compared this to *in vitro* calcite deposition on isolated intact eggshell membranes.

2. Materials and Methods

2.1. Reagents and Materials

Chemicals: Poly-L-glutamic acid (sodium salt) (15,000–50,000 mol wt), anhydrous sodium sulfate, methanol, tetrafluoroboric acid etherate, *N*-(3-dimethylaminopropyl)-*N'*-ethylcarbodiimide hydrochloride (EDC), *N*-hydroxysuccinimide (NHS), and lithium hydroxide were from Merck KGaA, (formerly Sigma-Aldrich), Darmstadt, Germany.

Plasticware: Falcon® polypropylene conical centrifuge tubes (Corning, Glendale, AZ, USA) and micro-bridges (Hampton Research, Laguna Niguel, CA, USA) were used.

2.2. Eggshell Membrane (ESM) Functionalization

Protocols for functionalization were adapted from Greene and Wuts [24]. ESM were obtained from commercial White Leghorn chicken eggs. Empty eggs were filled with 1% acetic acid solution for 30 min to detach the membrane from the shell, and then ESM were incubated for another 48 hours in 1% acetic acid solution to eliminate any remaining calcium carbonate crystals, washed three times in deionized water, and manually detached from the shell [25]. Strips, 3 mm wide × 20 mm long were trimmed off the isolated ESM. Functionalization of ESM with poly-glutamic acid is diagrammed in Figure 1, and the reaction was followed by Fourier Transform Infrared spectroscopy (FTIR) using a FTIR/FTNIR bench-top spectrometer (INTERSPEC 200-X, Interspectrum OÜ, Tartumaa, Estonia).

2.2.1. Protection of the Carboxyl Groups of Poly-glutamic Acid

Briefly, 15 mg of poly-L-glutamic acid sodium salt (P-Glu) was mixed with 7 mg of sodium sulfate and suspended in 10 mL of methanol in a 50-mL Falcon tube. Then, 2 mL of tetrafluoroboric acid etherate was added with a micropipette. The mixture was stirred at room temperature for 15 h. The resulting liquid was carefully removed by pipette suction, washed with 5 mL of methanol, centrifuged at 2500× *g* for 5 min, filtered with a Millipore filter, dried at room temperature, and saved properly [26]. This resulting product, where carboxyl groups from poly-glutamic acid were protected with methyl groups, was named P-Glu-CH₃.

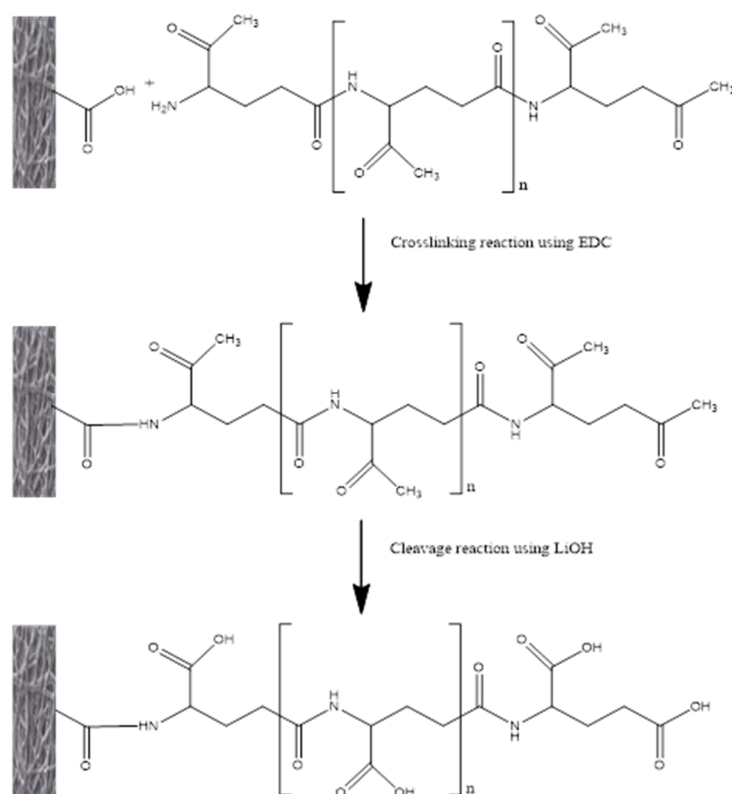


Figure 1. Diagrammatic representation of poly-glutamic acid coupling to eggshell membrane scaffold. Top to bottom: poly-glutamic acid carboxyl group protection, crosslinking of methyl carboxylate poly-glutamate to eggshell membrane, and cleavage of methyl groups to restore carboxylate groups to the poly-glutamic acid coupled to the eggshell membrane scaffold.

2.2.2. Crosslinking of P-Glu-CH₃ to Eggshell Membranes

ESM strips totaling 300 mg were introduced into a 5-mL Falcon tube and suspended in crosslinking solution consisting of: 10 mL of 0.1 M MES (2-*N*-morpholine-ethane sulfonic acid), 0.5 M NaCl, and pH 6.0 activation buffer, where 4 mg of EDC (1-ethyl-(3,3-dimethyl-aminopropyl)-carbodiimide) and 6 mg of NHS (*N*-hydroxysuccinimid) were added, stirred, and allowed to react for 15 min at room temperature. P-Glu-CH₃ was dissolved in 1 mL phosphate-buffered saline (PBS) pH 7.5 and added to the crosslinking solution. The reaction was allowed to proceed for 2 h at room temperature [27,28]. The ESM strips were filtered and washed twice with 3:1 methanol:water. This product was named P-Glu-CH₃ ESM strips.

2.2.3. Cleavage of Methyl Groups to Restore Carboxylate Groups

P-Glu-CH₃ ESM strips were suspended in 10 mL of 3:1 methanol:water, 240 mg of lithium hydroxide were added, and the reaction was allowed to proceed at 4 °C for 15 h [29]. Then the strips were filtered with ethanol on a Millipore filter. This active polycarboxylated EMS was named P-Glu ESM.

2.3. Calcium Carbonate Crystallization Experiments

The crystallization assay was based on a variation of the sitting drop method developed elsewhere [30]. Briefly, the assay consists of a chamber built with an 85-mm diameter plastic Petri dish having a central hole of 18 mm in diameter at the bottom, with the chamber glued to a plastic cylindrical vessel (50 mm in diameter and 30 mm in height) (Figure 2a). Calcium carbonate crystallization was done on micro-bridges located inside the chamber. The micro-bridge is a small

bridge (inverted U) manufactured from clear polystyrene, which contains a smooth, 35- μL capacity concave depression able to hold a volume of liquid, essentially a hemispherical micro-well, in the center of the top region of the bridge. Micro-bridges were filled with 35 μL of 200 mM calcium chloride dihydrate solution in 200 mM Tris buffer, pH 9.0. The cylindrical vessel contained 3 mL of 25 mM ammonium bicarbonate. One 3-mm wide X 20-mm long ESM or P-Glu ESM strip was deposited on the top of each micro-bridge with the mammillary side facing down in contact with the calcium chloride solution, leaving enough space between the contour of the strip and the perimeter of the micro-well to allow free diffusion from the chamber to the CaCl_2 solution (Figure 2b). Strips ends were attached to the micro-well edges with by double-sided tape. Five replicates of each experiment were carried out inside the chamber at 20 $^\circ\text{C}$ for 24 h. After the experiments, and before the ESM strips were taken out of the micro-bridges, the solution inside the micro-well was removed with a micropipette and replaced twice with distilled water, and then it was dehydrated with a 50% to 100 % ethanol gradient solution series. Then the ESM strips were removed, mounted on aluminum stubs with double-sided tape, air-dried for 24 h at room temperature, and coated with gold. After the crystallization assays, the ESM strips mounted on aluminum stubs were analyzed. Crystal morphology was observed and size was estimated on a Jeol JSM-IT300LV (Jeol USA, Inc., Peabody, MA, USA) scanning electron microscope (SEM) operated at 20 kV with an EDX AZTec Oxford detector. Ten randomized selected fields of the SEM micrographs of five replicates were used for calculating crystal number and size. Statistical analyses of crystal size and density were done with InfoStat 2014 (Córdoba, Argentina) software. For determining the type of data distribution, a Shapiro–Wilk test was used. The $p > 0.05$ statistical significance level between the control (ESM) and polycarboxylated eggshell membrane (P-Glu ESM) samples was analyzed by Student t test. Results are expressed as mean \pm SD.

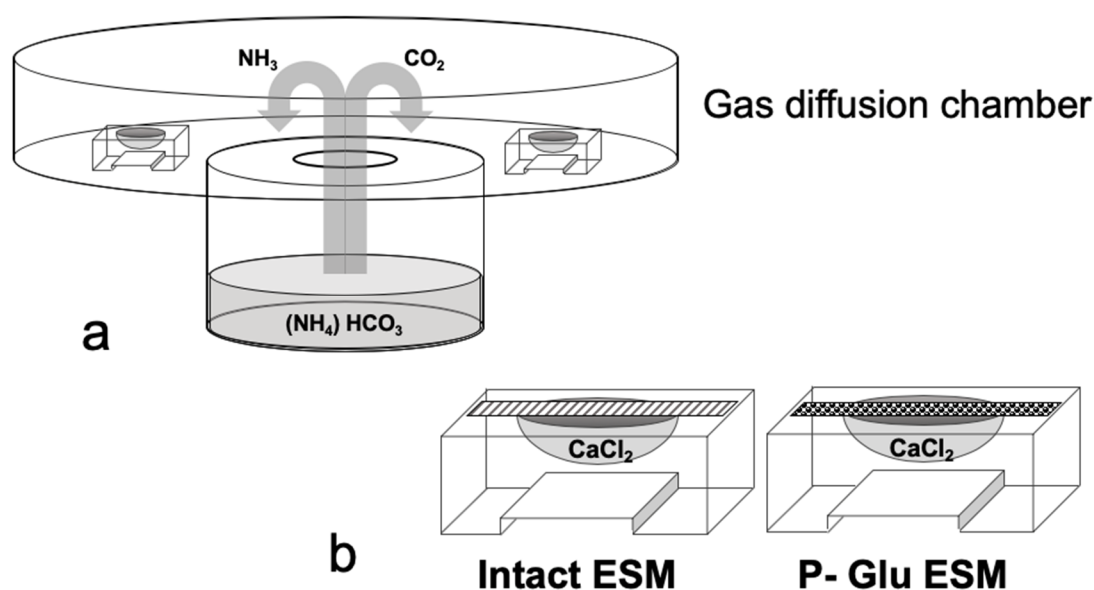


Figure 2. Diagram of the experimental crystallization chamber. (a) Gas diffusion chamber design, (b) location of the eggshell membrane strips on the top of the micro-bridges.

3. Results and Discussion

As expected, the main components of the ESM are carbon, hydrogen, nitrogen, oxygen, and sulfur. As has been shown elsewhere [31,32], the Fourier Transform Infrared (FTIR) spectrum of ESM (Figure 3) shows, in the region of higher wavenumbers, an intensive peak at 3271 cm^{-1} , which corresponds to the stretching mode of O–H and N–H groups. Peaks at 2923 and 2102 cm^{-1} correspond to the asymmetric stretching vibrations of the C–H bonds present in =C–H and =C–H₂ groups, while in the region with

lower wavenumbers, the peaks at 1628 cm^{-1} , 1531 cm^{-1} , and 1446 cm^{-1} represent the C=O stretching, N–H bending amide absorption bonds, and CH_2 scissoring bonds, respectively. Eggshell membranes coupled to methyl esterified poly-glutamate (P-Glu- CH_3 ESM) showed a similar spectrum to the intact eggshell membranes. However, when the methyl groups were cleaved from P-Glu- CH_3 ESM restoring the carboxylate groups, the FTIR spectrum showed a new peak at 1441 cm^{-1} indicative of absorption of COO^- symmetric stretching as described for pure poly- γ -glutamic acid [33,34]. After calculation of the absorbance integrated area of the P-Glu ESM FTIR spectrum (Figure 1) in the range of 1400 to 1800 cm^{-1} using a Gaussian model and a polynomial baseline of order 5, it was possible to theoretically estimate the unblocked carboxylic groups that were able to affect the CaCO_3 crystallization. In accordance with the empirical formula of poly-glutamic acid, considering a theoretical polydispersity index of 1, it contains a proportion of 4 carboxylic groups per 7 carbonyl groups, that is a quotient of 0.57. A Gaussian integrated area of -564.5346 was obtained, representing the carbonyl groups indistinctively derived from carboxylic or other sources. However, we found that the peak of 1441 cm^{-1} showed an integrated area of -230.7645 , representing the fraction of ionized carboxylate groups. Thus, the quotient of the ionized carboxylate groups divided by the total carbonyl groups is 0.41. By quotients comparison, the LiOH cleavage had an effectiveness of 71.9%.

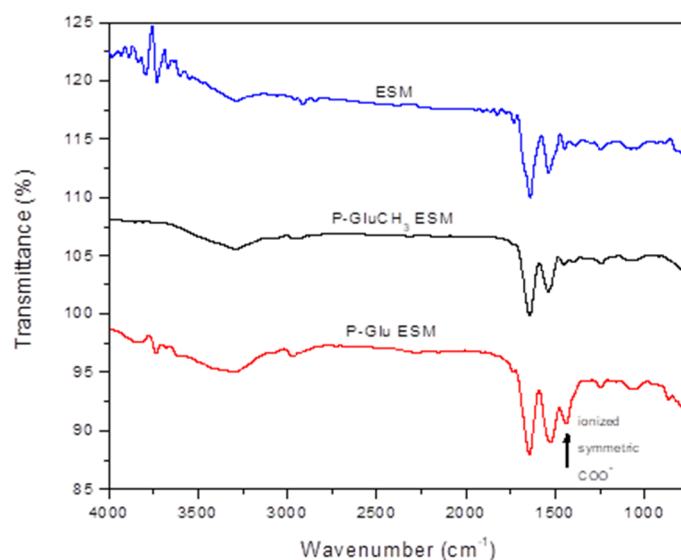


Figure 3. FTIR spectra of intact eggshell membrane (ESM), carboxyl group-protected poly-glutamic acid coupled to eggshell membrane (P-Glu- CH_3 ESM), and poly-glutamic acid coupled to eggshell membrane (P-Glu ESM). Ionized symmetric carboxylate groups are shown at 1441 cm^{-1} .

In our assay system, when calcium carbonate crystallization assays are done with a variation of the sitting drop method using micro-bridges inside a closed mini-chamber (Figure 2), but without any additive, CO_2 produced from $(\text{NH}_4)\text{HCO}_3$ interacts first with the surface of the hemispherical micro-well containing the CaCl_2 solution. Thus, under this condition, nucleation of CaCO_3 crystals occurs first at this interface, and after reaching a certain size, these crystals leave the surface and sink in the CaCl_2 solution, reaching the micro-bridge bottom and forming typical rhombohedral calcite crystals of different sizes probably due to a diffusion phenomenon of CO_2 in the calcium chloride solution (Figure 4). Hence, under this experimental condition, extreme caution must be taken when the eggshell membrane scaffold is used as an additive for driving heterogeneous nucleation on its surface. In fact, when an eggshell membrane strip is deposited on the bottom of the micro-bridge, it becomes very difficult to differentiate the crystals that are deposited by gravity on the eggshell membrane scaffold from those that grow bottom-up because of the nucleation and growth effect of the eggshell membrane proper. This, therefore, is the reason why ESM or P-Glu ESM strips were

placed on the top of each micro-bridge with the mammillary side facing down in contact with the calcium chloride solution. Under this condition, the effect of crystal deposition because of gravity is avoided, and the crystallization occurring on the eggshell membrane surface reflects the proper influence of the template. As shown in Figure 5, crystalline calcium carbonate aggregates occurred preferentially on mammillary sites of intact eggshell membranes (Figure 5a,c). This feature resembles very well what occurs during natural eggshell formation, where calcium carbonate deposition begins on the outer mammillary side of the eggshell membranes, closely associated with the negatively charged keratan-sulfate proteoglycan-rich mammillae, and then progresses in an upward direction. The final complex architecture of the eggshell calcified layer is the result of the interaction of calcium carbonate crystals with organic matrix molecules consisting of proteins and proteoglycans [11,15,35,36]. In contrast, when a poly-glutamic acid-functionalized eggshell membrane is used, large amounts of calcitic aggregates grow not only on mammillary sites but directly on the eggshell membrane fibers (Figure 5b,d). In fact, a threefold greater amount of crystals was grown on the poly-glutamic acid-functionalized eggshell membrane compared with the intact eggshell membrane: 2334 ± 677 vs. 674 ± 213 crystals per square millimeter, respectively (Figure 6a). However, there is no significant difference between the size of the crystals formed on both scaffolds: 10.49 ± 2.9 vs. 10.66 ± 4.32 μm , respectively (Figure 6b). Therefore, it is reasonable to conclude that the addition of poly-carboxylated groups onto eggshell membranes increases the number of surface nucleation sites but, because of the inorganic ion concentration, the crystal size reached at 24 h is not affected.

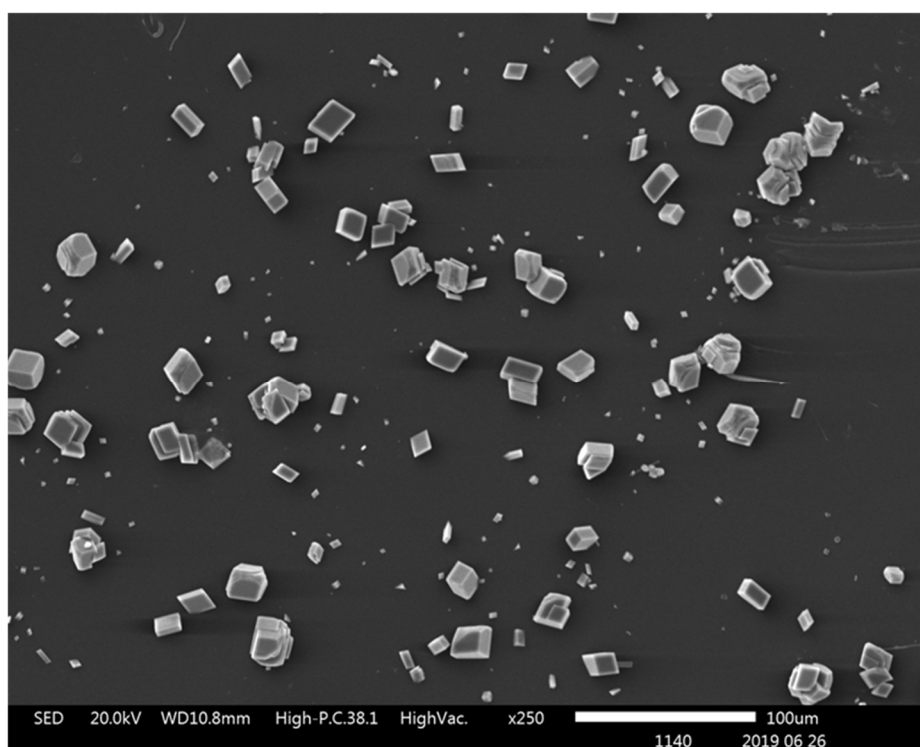


Figure 4. Representative scanning electron microscopy (SEM) observation of normal rhombohedral calcite crystals grown on the bottom of the micro-bridge under the experimental conditions but in the absence of any additive.

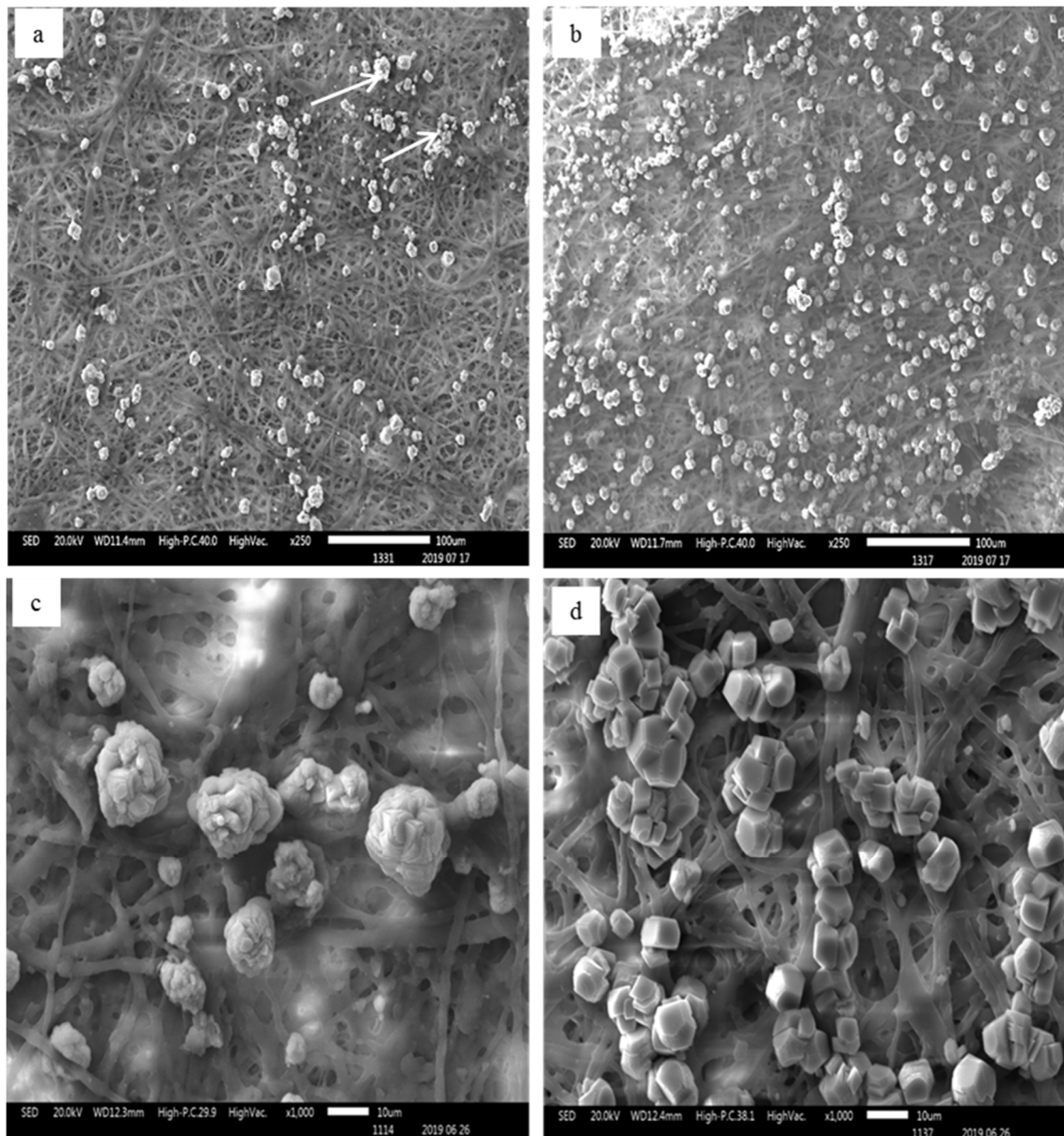


Figure 5. Representative SEM observation of calcite crystals grown on intact eggshell membrane (a,c) vs. growing on poly-glutamic acid-coupled eggshell membrane (b,d). Different kinds of crystal aggregations are shown. Arrows illustrate some mammillary sites.

Our results apparently disagree with other findings in which poly-glutamic acid associated with eggshell membranes induced an aragonite phase [37]. However, these authors did the experiments under different and not directly comparable conditions such as preadsorbing rather than chemically coupling the poly-glutamic acid to the eggshell membranes, and also using a different calcification protocol. Additionally, different effects on calcium carbonate crystallization have been described when poly-glutamic acid is not supported on a solid scaffold but instead is incorporated as an additive in solution [38]. Under these conditions, the addition of poly-glutamic acid to the CaCO_3 precipitation solution substantially inhibits both nucleation and crystal growth of stable calcite compared with the unstable vaterite polymorph, probably as a consequence of kinetic constraints through a stronger binding of acidic polypeptide by the calcite surfaces than by the vaterite surfaces [38]. Therefore, care must be taken when the effects of additives are compared with additives incorporated in solution or,

forming part of a copolymer or hydrogel, adsorbed or chemically coupled to a solid scaffold in an inorganic precipitation solution at equivalent saturation concentrations.

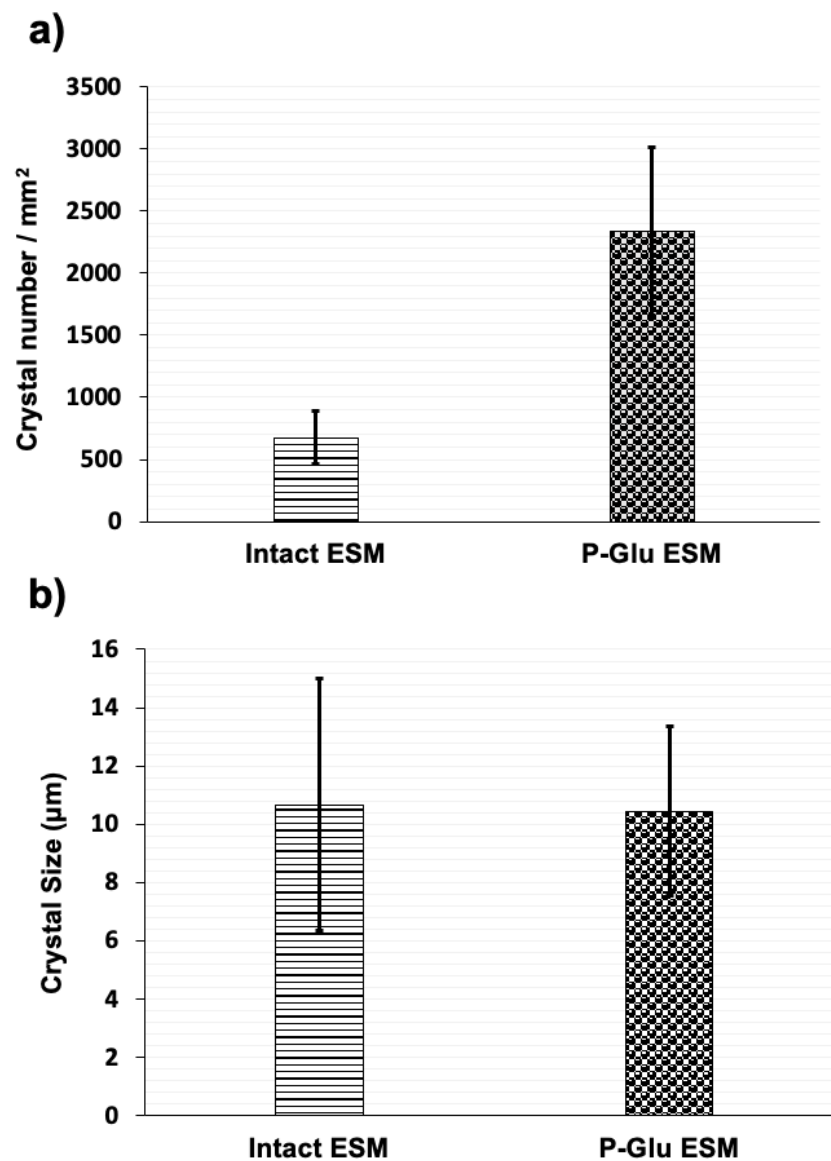


Figure 6. Statistical analysis (mean \pm SD) of the density (a) and size (b) of calcite crystals grown on intact eggshell membrane or on poly-glutamic acid-coupled eggshell membrane.

4. Conclusions

Based on the results obtained in this study, it seems that widespread poly-glutamic negatively charged sites attached to the eggshell membrane fibers compete with the natural mammillary keratan sulfate negatively charged sites for calcite nucleation and growth under equivalent experimental conditions. This study also offers a possible explanation for the mechanism of nucleation and crystal growth of calcium carbonate and a possible role of negatively charged chemical groups coupled on a solid substrate on calcium carbonate biomineralization.

Author Contributions: Conceptualization, J.L.A.; methodology, A.N.-C., N.B.; investigation, K.S., L.O., M.S.F., J.I.A.; writing—original draft, review and editing, J.L.A., M.S.F., J.I.A.; funding acquisition, J.L.A. All authors have read and agreed to the published version of the manuscript.

Funding: The research described in this paper was financially supported by the Chilean Government National Agency of Research and Development (ANID), grant Fondecyt N° 1180734.

Acknowledgments: The authors would like to thank Rocío Orellana of the Scanning Electron Microscopy Laboratory, Faculty of Dentistry, University of Chile. The authors would also like to thank David A. Carrino (Cleveland, OH) for providing insightful comments on the manuscript language style, spelling and scientific expertise suggestions.

Conflicts of Interest: The authors declare no conflict of interest.

References

1. Lowenstam, H.A.; Weiner, S. *On Biomineralization*; Oxford University Press: Oxford, UK, 1989.
2. Mann, S.; Webb, J.; Williams, R.J.P. *Biomineralization*; VCH: Weinheim, Germany, 1989.
3. Simkiss, K.; Wilbur, K.M. *Biomineralization*; Academic Press: San Diego, CA, USA, 1989.
4. Baeuerlein, E. *Biomineralization*; Wiley-VCH: Weinheim, Germany, 2000.
5. Mann, S. *Biomineralization*; Oxford University Press: Oxford, UK, 2001.
6. Baeuerlein, E. *Handbook of Biomineralization: Biological Aspects and Structure Formation*; Wiley-VCH: Weinheim, Germany, 2007.
7. Arias, J.L.; Fernández, M.S. *Biomineralization: From Paleontology to Materials Science*; Editorial Universitaria: Santiago, Chile, 2007.
8. Endo, K.; Kogure, T.; Nagasawa, H. *Biomineralization: From Molecular and Nano-Structural Analyses to Environmental Science*; Springer Nature Singapore Pte Ltd.: Singapore, 2018.
9. Fernández, M.S.; Montt, B.; Ortiz, L.; Neira-Carrillo, A.; Arias, J.L. Effect of Carbonic Anhydrase Immobilized on Eggshell Membranes on Calcium Carbonate Crystallization In Vitro. In *Biomineralization: From Molecular and Nano-Structural Analyses to Environmental Science*; Endo, K., Kogure, T., Nagasawa, H., Eds.; Springer Nature Singapore Pte Ltd.: Singapore, 2018; pp. 31–37.
10. Fernández, M.S.; Araya, M.; Arias, J.L. Eggshells are shaped by a precise spatio-temporal arrangement of sequentially deposited macromolecules. *Matrix Biol.* **1997**, *16*, 13–20. [[CrossRef](#)]
11. Fernández, M.S.; Moya, A.; López, L.; Arias, J.L. Secretion pattern, ultrastructural localization and function of extracellular matrix molecules involved in eggshell formation. *Matrix Biol.* **2001**, *19*, 793–803. [[CrossRef](#)]
12. Arias, J.L.; Fink, D.; Xiao, S.Q.; Heuer, A.H.; Caplan, A.I. Biomineralization and eggshells: Cell-mediated acellular compartments of mineralized extracellular matrix. *Int. Rev. Cytol.* **1993**, *145*, 217–250. [[PubMed](#)]
13. Simons, P.C.M. Ultrastructure of the hen eggshell and its physiological interpretation. *Agric. Res. Repts.* **1971**, *758*, 1–90.
14. Nys, Y.; Hincke, M.T.; Arias, J.L.; Garcia-Ruiz, J.M.; Solomon, S.E. Avian eggshell mineralization. *Poult. Avian Biol. Rev.* **1999**, *10*, 143–166.
15. Rao, A.; Arias, J.L.; Cölfen, H. On mineral retrosynthesis of a complex biogenic scaffold. *Inorganics* **2017**, *5*, 16. [[CrossRef](#)]
16. Panhéleux, M.; Bain, M.; Fernández, M.S.; Morales, I.; Gautron, J.; Arias, J.L.; Solomon, S.; Hincke, M.; Nys, Y. Organic matrix composition and ultrastructure of eggshells: A comparative study. *Br. Poultry Sci.* **1999**, *40*, 240–252. [[CrossRef](#)]
17. Arias, J.L.; Mann, K.; Nys, Y.; García-Ruiz, J.M.; Fernandez, M.S. Eggshell growth and matrix macromolecules. In *Handbook of Biomineralization*; Baeuerlein, E., Ed.; Wiley-VCH: Weinheim, Germany, 2007; Volume 1, pp. 309–327.
18. Hincke, M.T.; Nys, Y.; Gautron, J.; Mann, K.; Rodriguez-Navarro, A.B.; McKee, M.D. The eggshell: Structure, composition and mineralization. *Front. Biosci.* **2012**, *17*, 1266–1280. [[CrossRef](#)]
19. Arias, J.L.; Fernandez, M.S.; Dennis, J.E.; Caplan, A.I. Collagens of the chicken eggshell membranes. *Connect. Tissue Res.* **1991**, *26*, 37–45. [[CrossRef](#)]
20. Du, J.; Hincke, M.T.; Rose-Martel, M.; Hennequet-Antier, C.; Brionne, A.; Cogburn, L.A.; Nys, Y.; Gautron, J. Identifying specific proteins involved in eggshell membrane formation using gene expression analysis and bioinformatics. *BMC Genom.* **2015**, *16*, 792. [[CrossRef](#)]
21. Cordeiro, C.M.M.; Hincke, M.T. Quantitative proteomics analysis of eggshell membrane proteins during chick embryonic development. *J. Proteom.* **2015**, *130*, 11–25. [[CrossRef](#)] [[PubMed](#)]

22. Britton, W.; Hale, K. Amino acid analysis of shell membranes of eggs from young and old hens varying in shell quality. *Poultry Sci. J.* **1976**, *56*, 865–871. [[CrossRef](#)]
23. Arias, J.L.; Carrino, D.A.; Fernandez, M.S.; Rodriguez, J.P.; Dennis, J.E.; Caplan, A.I. Partial biochemical and immunohistochemical characterization of avian eggshell extracellular matrices. *Arch. Biochem. Biophys.* **1992**, *298*, 293–302. [[CrossRef](#)]
24. Greene, T.W.; Wuts, P.G.M. *Protective Groups in Organic Synthesis*, 2nd ed.; John Wiley & Sons: New York, NY, USA, 1991.
25. Arias, J.I.; Gonzalez, A.; Fernandez, M.S.; Gonzalez, C.; Saez, D.; Arias, J.L. Eggshell membrane as a biodegradable bone regeneration inhibitor. *J. Tiss. Eng. Regen. Med.* **2008**, *2*, 228–235. [[CrossRef](#)] [[PubMed](#)]
26. Albert, R.; Danklmaier, J.; Honig, H.; Kandolf, H. A simple and convenient synthesis of β -aspartates and γ -glutamates. *Synthesis* **1987**, *7*, 635–637. [[CrossRef](#)]
27. Grabarek, Z.; Gergely, J. Zero-length crosslinking procedure with the use of active esters. *Anal. Biochem.* **1990**, *185*, 131–135. [[CrossRef](#)]
28. Enrione, J.; Díaz-Calderón, P.; Weinstein-Oppheimer, C.R.; Sánchez, E.; Fuentes, M.; Brown, D.L.; Herrera, H.; Acevedo, C.A. Designing a gelatin/chitosan/hyaluronic acid biopolymer using thermophysical approach for use in tissue engineering. *Bioproc. Biosyst. Eng.* **2013**, *36*, 1947–1956. [[CrossRef](#)] [[PubMed](#)]
29. Corey, E.J.; Székely, L.; Shiner, C.S. Synthesis of 6, 9 α -oxido-11 α , 15 α . dihydroxyprosta-(E)5, (E)13-dienoic acid, an isomer of PGI₂ (vane's PGX). *Tetrahedron Lett.* **1977**, *40*, 3529–3532. [[CrossRef](#)]
30. Dominguez-Vera, J.M.; Gautron, J.; Garcia-Ruiz, J.M.; Nys, Y. The effect of avian uterine fluid on the growth behavior of calcite crystals. *Poultry Sci.* **2000**, *6*, 901–907. [[CrossRef](#)]
31. Kaur, N.; Thakur, H.; Pathak, S.; Prabhakar, N. Acetylcholinesterase immobilised eggshell membrane-based optical biosensor for organophosphate detection. *Int. J. Environ. Anal. Chem.* **2015**, *95*, 1134–1147. [[CrossRef](#)]
32. Hsieh, S.; Chou, H.H.; Hsieh, C.W.; Wu, D.C.; Kuo, C.H.; Lin, F.H. Hydrogen peroxide treatment of eggshell membrane to control porosity. *Food Chem.* **2013**, *141*, 2117–2121. [[CrossRef](#)] [[PubMed](#)]
33. Khalil, I.R.; Khechara, M.P.; Kurusamy, S.; Armesilla, A.L.; Gupta, A.; Mendrek, B.; Khalaf, T.; Scandola, M.; Focarete, M.L.; Kowalczyk, M.; et al. Poly-gamma-glutamic acid (γ -PGA)-based encapsulation of adenovirus to evade neutralizing antibodies. *Molecules* **2018**, *23*, 2565. [[CrossRef](#)] [[PubMed](#)]
34. Wang, L.-L.; Chen, J.-T.; Wang, L.-F.; Wu, S.; Zhang, G.-Z.; Yu, H.-Q.; Ye, X.-D.; Shi, Q.-S. Conformations and molecular interactions of poly- γ -glutamic acid as a soluble microbial product in aqueous solutions. *Sci. Rep.* **2017**, *7*, 12787. [[CrossRef](#)] [[PubMed](#)]
35. Fernandez, M.S.; Escobar, C.; Lavelin, I.; Pines, M.; Arias, J.L. Localization of osteopontin in oviduct tissue and eggshell during different stages of the avian egg laying cycle. *J. Struct. Biol.* **2003**, *43*, 171–180. [[CrossRef](#)]
36. Fernandez, M.S.; Passalacqua, K.; Arias, J.L.; Arias, J.L. Partial biomimetic reconstitution of avian eggshell formation. *J. Struct. Biol.* **2004**, *148*, 1–10. [[CrossRef](#)]
37. Ajikumar, P.K.; Lakshminarayanan, R.; Valiyaveetil, S. Controlled deposition of thin films of calcium carbonate on natural and synthetic templates. *Cryst. Growth Design.* **2004**, *4*, 331–335. [[CrossRef](#)]
38. Njegić-Džakula, B.; Falini, G.; Brečević, L.; Skoko, Ž.; Kral, D. Effects of initial supersaturation on spontaneous precipitation of calcium carbonate in the presence of charged poly-L-amino acids. *J. Colloid Interf. Sci.* **2010**, *343*, 553–563. [[CrossRef](#)]

